

First-principles study of optical aspects of penta-graphene monolayer under strain effects

Hamidreza Alborznia

Department of Physics, Center of Basic Science, Khatam Ol-Anbia (PBU) University, Tehran, Iran

E-mail: hamidrezaalborznia@gmail.com

Received 09 April 2024; accepted (revised) 30 August 2024

In this study, based on the first-principles calculations using the Density Functional Theory (DFT) employing Wien2k computing codes, the optical properties of penta-graphene such as the joint density of states, the real and imaginary part of the complex dielectric function, absorption, and reflectivity spectrum under special conditions such as strain effects, are studied. The behavior of the optical aspects of penta-graphene is analyzed. It can be concluded that this monolayer is suitable for use in designing optoelectronic devices, especially as sensors under the proposed conditions.

Keywords: First-principles calculations, Density Functional Theory (DFT), Optical properties, Strain effects

Carbon as a unique element, due to the covalent bond of each atom with its type or other types of atoms, has caused the creation of unlimited and very diverse carbon structures and nanostructures. Carbon allotropes such as nanofibers and nanostructures have an important contribution to nanotechnologies. The diverse and unique physicochemical allotropes of nanofibers and carbon structures have made these structures play a large role in modern and advanced technologies. Predicting new carbon compounds and structures with new electronic and optical aspects can play a significant role in constructing and producing new electronic and optical tools. The discovery of graphene has become a turning point for the beginning of extensive research on the physical properties of this carbon allotrope, such as dynamic, electronic, and optical properties for designing electronic and optoelectronic devices. Various types of two and three-dimensional carbon allotropes were discovered and predicted in different classifications. Some of the physical aspects such as the dynamic, electronic, and optical properties were investigated¹⁻¹⁸. In this study, optical properties such as the joint density of states, the real and imaginary part of the complex dielectric function, absorption, and reflectivity spectrum of penta-graphene are investigated under strain effects based on the method of first-principles calculations using density functional theory (DFT), and changing the behavior of the optical aspects of this monolayer are analyzed.

Calculation method

To calculate the optical properties of the carbon nano-allotrope under applied conditions, density functional theory (DFT), from the Wien2k computational code¹⁹ is used. Wien2k is a computational code for processing crystalline and molecular structures and nanostructures with the full potential approximation and software based on the linear amplified flat wave method with the full potential, which is considered one of the most accurate methods for calculating the energy band structure. Using this software, it is possible to simulate crystal structures and nanostructures and predict many of their physical properties. Also, by solving the Kohn-Sham equations in a crystal lattice, the electronic and magnetic structure and other aspects such as charge and spin distribution are obtained. This calculation package determines the structural properties of crystals and molecules in the presence of impurity and under various approximations such as GGA, and LDA which can solve problems by the application of mean-field approximations, such as the Hubbard parameter. This study analyzes the optical properties following carbon nano-allotrope using the Wien2k computational code with the GGA generalized gradient approximation by selecting $1 \times 12 \times 12$ and $1 \times 25 \times 25$ meshing. For inverted points in the first Brillion zone, the (PBE) method is used²⁰, and for the calculations of exchange-correlation interactions, the Monkhorst-

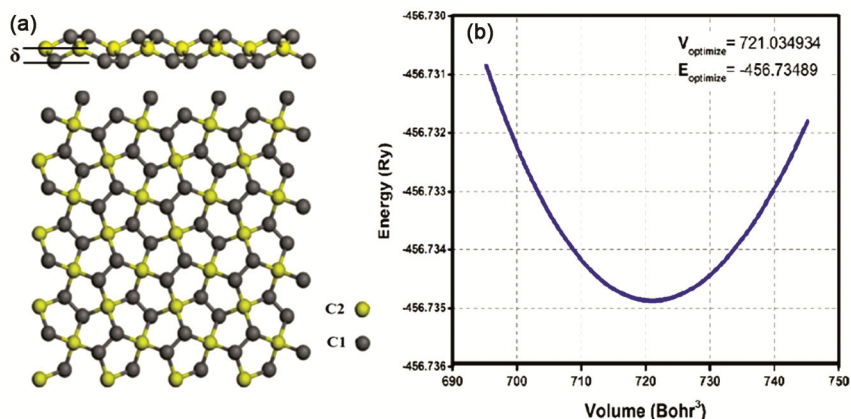


Fig. 1 — (a) Top and side views of the penta-graphene supercell (b) Energy vs. volume unit cell of penta-graphene

Peck approximation is used²². Calculation input parameters $RMTK_{\max} = 7$, $G_{\max} = 14 \text{ Ry}^{1/2}$, $I_{\max} = 10$, and separation energy of the nucleus from the valence electrons equal to 8 Ry are selected and the calculations are performed with non-polar settings. Also, Kramers-Kronig relations and the random phase approximation method (RPA) are used to obtain different components of the dielectric function²³.

Results and Discussion

Structural properties

A new two-dimensional allotrope of carbon, called penta-graphene, was predicted as an indirect bandgap semiconductor in 2015¹¹. Then, by using DFT, the energy structure and electronic properties of the two-dimensional penta-graphene nanostructure have been studied to understand the feasibility of synthesizing this nanostructure and its application in Nano-electronics. In this section, based on the principles of basic calculations related to the DFT, in line with new research, the optical properties of the optimized structure of the penta-graphene unit cell under strain due to vertical compressive strain in the Z direction are investigated¹². The final results show that according to the considered conditions, the desired nanostructure can be effective in the design of multi-purpose electro-optical devices.

The two-dimensional crystal nanostructure of penta-graphene shown in Fig. 1, has space group no. 113 and $P-421m$ with a tetragonal lattice consisting of two types of carbon-carbon bond lengths (C1 and C2), where the atomic layer C2 with sp^3 hybridization is located between two layers of C1 with sp^2 hybridization. According to Fig. 1, the constants of the penta-graphene network have been optimized using the thermodynamic mode of Birch-Murganjan equations²⁴.

Table 1 — Optimized structural data of Penta-graphene by PBE-GGA method.

Method	Optimized lattice (Å)	Strain (Å)	Bond length (Å)	$E_{\text{opt}}(\text{Ry})$
PBE-GGA	$a = b = 3.649$	$\delta = 0.589$	C1-C2 = 1.543 C1-C1 = 1.342	-456.735

$$E(V) = E_0 + \frac{9B_0V_0}{16} \left\{ \left[\left(\frac{V_0}{V} \right)^{2/3} - 1 \right]^3 B'_0 \right\} + \frac{9B_0V_0}{16} \left\{ \left[\left(\frac{V_0}{V} \right)^{2/3} - 1 \right]^2 \left[6 - 4 \left(\frac{V_0}{V} \right)^{2/3} \right] \right\} \quad \dots(1)$$

In Equation (1), the optimum volume energy is obtained with the lattice parameters (a, b) where B'_0 concerns the bulk modulus under pressure, B_0 is the modulus in zero pressure, and V_0 is the primary volume. Fig. 1 (a), shows the top and side views of the Penta-graphene 2D crystal supercell, and (b) indicates the volume vs energy curve for the penta-graphene. The curve's minimum point in Fig. 1(b) shows the optimized volume in the least energy of the unit cell. From the obtained equilibrium volume, the optimized lattice parameter is proposed as $a = b = 3.649 \text{ \AA}$, and the thickness between each upper and lower layer of the C1 atom is called the strain (δ), which is equal to 0.589 \AA . Consequently, the total thickness of the 2D Penta-graphene nanosheet is 1.178 \AA .

Table 1 demonstrates the calculated optimized structural data of Penta-graphene such as lattice parameter, strains constant, bond length, and optimized energy by using the PBE-GGA approximation method¹².

Results of the investigation of the structural properties of this 2D carbon allotrope indicate that optimized penta-graphene nanostructure is known as

an indirect band gap semiconductor, it has structural data following previous studies^{27,28}. Also according to Fig. 2, the band gap and total energy are calculated under strain reduction up to 12%. The results show that when the strain constant is reduced, the total energy and consequently, stability of the system slightly decreases according to the blue curve in Fig. 2. The band gap shifts under the effect of strain variation shown by the violet curve in Fig. 2, which illustrates by imposing vertical stress, the band gap of penta-graphene is reduced.

Optical properties

In this part, some significant optical properties such as joint density of states, real and imaginary parts of the complex dielectric function, absorption, reflectivity spectrum, and energy loss, of the penta-graphene, in optimal state and strain variation condition up to 12 percent, are examined in the 0-30 eV energy range. Taking into account the fact that to make variations in the strain, it is necessary to apply stress in the vertical direction on the nanosheet, the optical properties in the Z polarization direction are investigated and plotted.

The joint density of states (joint DOS) of the optical inter-band transitions from the occupied states to the unoccupied states is investigated and shown in Fig. 3. This figure illustrates the joint DOS spectrum of the penta-graphene in the Z direction, without stress and under vertical stress conditions with 4, 8, and 12 percent to reduce strain constant. Fig. 3 shows that the joint DOS spectrum decreases with application stress in the nanomaterial. According to Fig. 3, due to the active stress, the strain parameter decreases in the Z-direction. In such a way that the sharp peak with the energy of about 11 eV in the non-stressed state, with stress, applied up to 12 percent on the penta-graphene, decreases the slope and moves towards the energy of about 14 eV.

Complex dielectric function, which consists of two parts, real and imaginary components as an operational factor to recognize all optical aspects such as absorption and reflectivity spectrum, is given by the following equation²⁵:

$$\epsilon_{complex} = \Re + i\Im \epsilon \quad \dots (2)$$

The real component of the dielectric function obtained using the Kramers-Kronig relation is as follows:

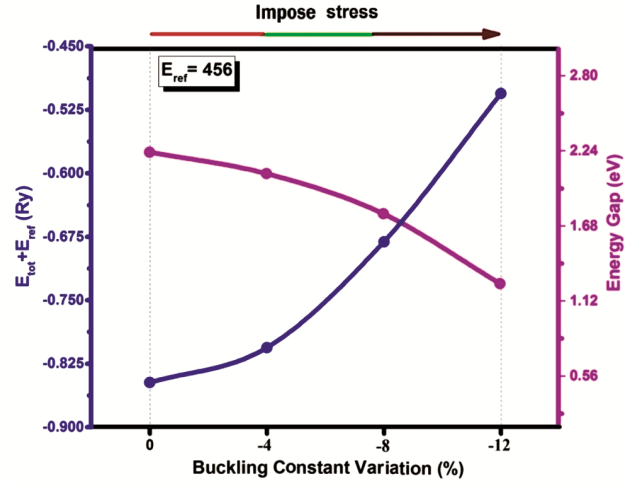


Fig. 2 — Band gap and total energy variation of penta-graphene under the strain effects

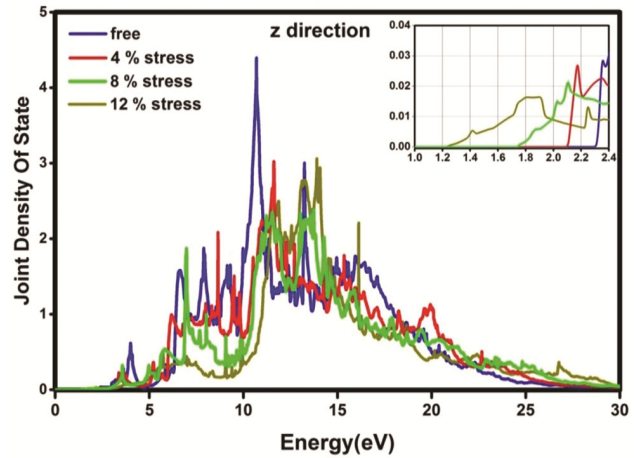


Fig. 3 — Joint Density of States (DOS) of the penta-graphene under stress condition.

$$\Re \epsilon^{\alpha\beta}(\omega) = \delta_{\alpha\beta} + \frac{2}{\pi} Pr. \int_0^{\infty} \frac{\Im \epsilon^{\alpha\beta}(\omega')}{\omega'^2 - \omega^2} \omega' d\omega' \quad \dots (3)$$

Where *Pr.* indicates the Cauchy principal value. Also, the effective factor in the inter-band optical transmissions between occupied (*ik*) and unoccupied electron states (*fk*) can be considered as the imaginary part of the complex dielectric function, the equation of which is:

$$\Im \epsilon^{\alpha\beta}(\omega) = \frac{4\pi e^2}{m^2 \omega^2} \sum_{i,j} \int \frac{2d^3k}{(2\pi)^3} | \langle ik | P_{\alpha} | fk \rangle |^2 f_i^k (1 - f_f^k) \delta(E_f^k - E_i^k - \hbar\omega) \quad \dots (4)$$

The real and imaginary plots of the dielectric function related to the penta-graphene in the Z direction, without stress and under vertical stress conditions with 4, 8, and 12 percent to reduce strain

constant, are displayed in Fig. 4 and, Fig. 5, respectively. As shown in Fig. 4, a sharp peak of transition occurred at about 6 eV in the non-stressed state, which decreases by increasing the stress up to 12%. Next sharp peaks are formed for modes affected by buckling for stresses of 8 and 12 percent, at higher energies in the range of 10 to 12 eV. Also According to Fig. 5, by applying stress in the imaginary part, in addition to reducing the peak of transition in the energy of about 10 eV, we see a rebound of transition peaks for stress states of 8 and 12 percent in energy of about 13 to 14 eV. These indicate the matching of the optical and electronic behaviors of this semiconductor under these conditions.

Two important aspects for the exploration of optical properties are undoubtedly absorption and reflectivity. Fig. 6 and Fig. 7 respectively, illustrate the 2D nanostructure of the penta-graphene absorption and reflectivity spectrums in the Z

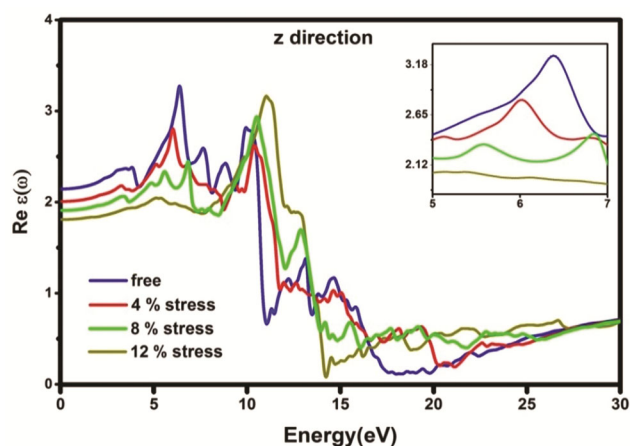


Fig. 4 — Real part plot of the dielectric function of the penta-graphene under stress condition

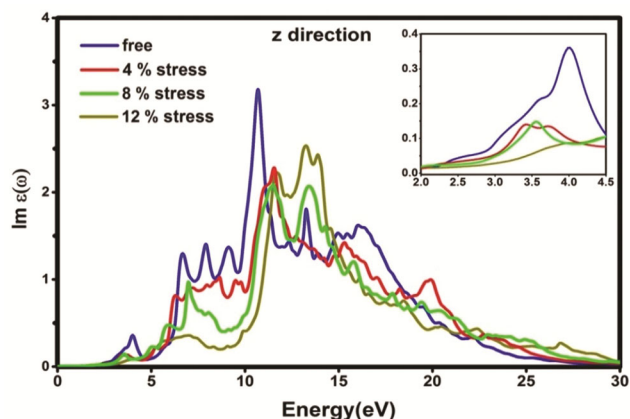


Fig. 5 — Imaginary part of the dielectric function of the penta-graphene under stress

direction, which are affected by changes in strain on this material by applying stresses with values of zero, 4, 8, and 12 percent. According to the figures, the absorption and reflectivity spectrums, from visible light energy to about 11 eV, are reduced by applying stresses up to 12%. This trend continues for a 4% stress state for higher optic energies up to 30 eV. But in energies between 13 – 15 eV for states of 8 and 12% stress, a rapid rise in the absorption and reflectivity amplitudes is observed by creating sharp peaks at 14 eV. These changes in optical behavior in these conditions are related to the electronic behaviors of this material, in the transformation of the indirect band into a direct band semiconductor, along with reducing the band gap.

At the end of this section, the energy loss spectrum (ELOSS) of penta-graphene has been examined under the conditions of this study. According to Fig. 8, the energy loss spectrum of this structure under compressive strain is relatively reduced by 8%. But at 12% strain reduction, sudden and rapid changes occur

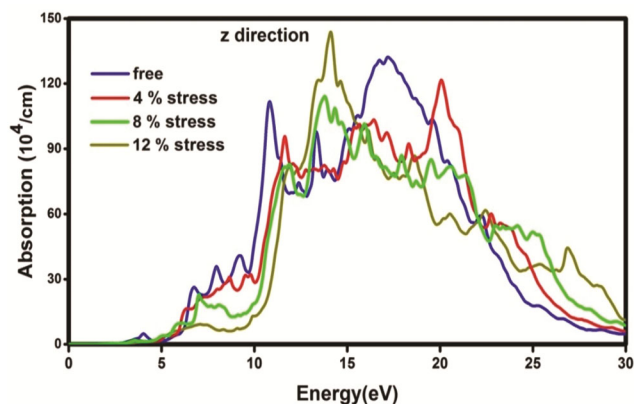


Fig. 6 — The absorption of the penta-graphene under strain stresses

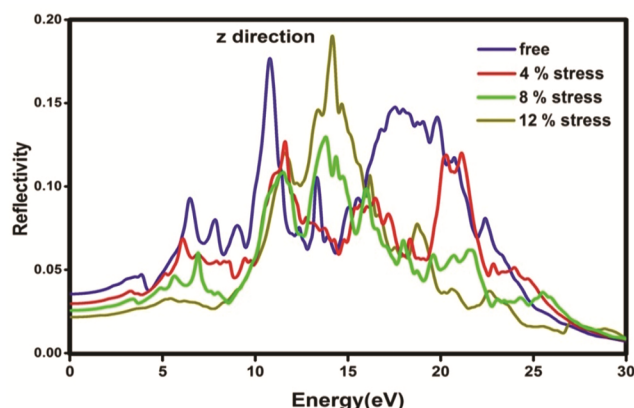


Fig. 7 — Reflectivity spectrum of the penta-graphene under strain stresses

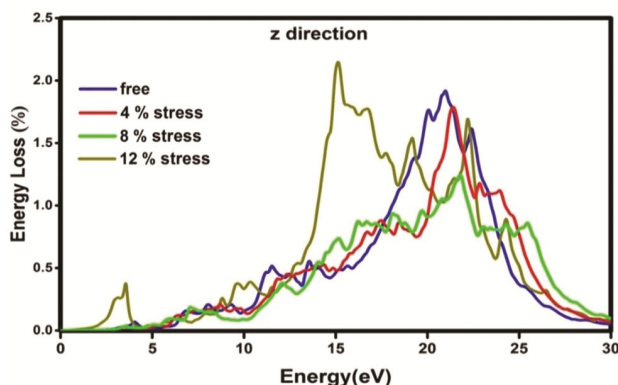


Fig. 8 — Energy loss spectrum of the penta-graphene under strain conditions

in the sharp peak, which indicates the plasma frequency of the structure, which shifts from the energy of 21 to 22 electron volts to the energy of 15 eV.

Conclusions

To summarize this study, as a new approach and research, the optical aspects of penta-graphene were investigated by first-principles calculation within the framework of density functional theory (DFT) using the Wien2k computational code. The optical properties of penta-graphene as 2D carbon nanostructure under strain conditions show a relative reduction in optical spectrums up to 4% strain, and also for 8 and 12% strains, the behavioral change is observed in optical properties, indicating well-matched properties with the electronic ones under these conditions. Finally, it can be concluded that these nanostructures are suitable for use in designing optoelectronic devices, especially as sensors under the proposed conditions.

Acknowledgments

This study is supported by Khatam Ol-Anbia University, Tehran, Iran. Hamidreza Alborznia would

like to thank Fateme Afrashte, and Alireza Alborznia for their interest in this work.

References

- 1 a) Rao C N R, H S S Matte & U Maitra, *Ange ChemieInt Edi*, 52 (2013) 13162.; b) Diederich F & Kivala M, *Adv Mat*, 22 (2010) 803.
- 2 Hirsch A, *Nat Mat*, 9 (2010) 868.
- 3 Li Q, Ma Y, Oganov A R, Wang H, Wang H, Xu Y, Cui T, Mao H-K & Zou G, *Phy Rev Lett*, 102 (2009) 175506.
- 4 Umemoto K, Wentzcovitch R M, Saito S & Miyake T, *Phy Rev Lett*, 104 (2010) 125504.
- 5 Wang J-T, Chen C & Kawazoe Y, *Phy Rev Lett*, 106 (2011) 075501.
- 6 Zhao Z, Xu B, Zhou X-F, Wang L-M, Wen B, He J, Liu Z & Wang H-T & Tian Y, *Phy Rev Lett*, 107 (2011) 215502.
- 7 Sheng X-L, Q-B Yan, F Ye, Q-R Zheng, G Su, *Phy Rev Lett*, 106 (2011) 155703..
- 8 Li D, Bao K, Tian F, Zeng Z, He Z, Liu B, Cui T, *Phy Chem Chem Phy*, 14 (2012) 4347.
- 9 C. He, L. Sun, C. Zhang, X. Peng, K. Zhang, J. Zhong, *PhyChemChemPhy*, 14 (2012) 8410.
- 10 Alborznia H, *Surface Rev Lett*, 29 (2022) 2250078.
- 11 Zhang S, Zhou J, Wang Q, Chen X, Kawazoe Y & Jena P, *Proc Natl AcadSci*, 112 (2015) 2372.
- 12 Alborznia H, Naseri M & Fatahi N, *SuperlattMicrostruc*, 133 (2019) 106217.
- 13 Karlický F & Turoň J, *Carbon*, 135 (2018) 134.
- 14 Alborznia H, Naseri M & Fatahi N, *Optik*, 180 (2019) 125.
- 15 Hoat D M, Amirian S, Alborznia H, Laref A, Reshak A H & Naseri M, *Indian J Phy*, 95 (2021) 2365
- 16 Alborznia H, *Int J Mod Phy B*, 38 (2024) 2450085.
- 17 Alborznia H & Mohammadi S T, *Indian J Phy*, 32 (2022) 3117.
- 18 Alborznia H R & Mohammadi S T, *Bull Mater Sci*, 44 (2021) 180.
- 19 Alborznia H, Amirian S & Naziradeh M, *Opt Quant Elec*, 54 (2022) 608.
- 20 Perdew J P, Burke K & Ernzerhof M, *Phys Rev Lett*, 77 (1996) 3865.
- 21 Heyd J, Scuseria G E & Ernzerhof M, *J Chem Phys*, 118 (2003) 8207.
- 22 H J Monkhorst & J D Pack, *Phy Rev B*, 13 (1976) 5188.
- 23 H Ehrenreich & M H Cohen, *Phys Rev*, 115 (1959) 786.
- 24 Birch F, *J Geophys Res B*, 83 (1978) 1257.
- 25 Abt R, Ambrosch-Draxl C & Knoll P, *Phys B: Cond Matt*, 194 (1994) 1451.